



Multi-level Image Enhancement for Pulmonary Tuberculosis Analysis

Chandrika V.¹, Parvathi C.S²., and P. Bhaskar³

Department of Instrumentation Technology,
Gulbarga University P G. Centre, Yeragera – 584 133.
Raichur, Karnataka, India
crgolds@rediffmail.com

ABSTRACT

The paper presents the task of auto-detecting the tiny nodules, which will help to get more information of pulmonary tuberculosis (TB). We apply two image processing technique into lung tissue information recognition. (1) A repetitive smoothing-sharpening technique is proposed and its impact is assessed to beneficially enhance X-ray lung images. (2) The ridge detection algorithm is going to diagnose indeterminate nodules correctly, allowing curative resection of early-stage malignant nodules and avoiding the morbidity and mortality of surgery for benign nodules. The proposed technique is tested on lung X-ray images. Results show that the proposed methodology has high potential to advantageously enhance the image contrast hence giving extra aid to radiologists to detect and classify TB.

Keywords: X-ray Lung Image Enhancement, Hybrid Image Enhancement, Repetitive Image Enhancement, Canny Edge Detection, Laplacien Filtering, Wavelet Transformation, Tuberculosis Cavities

1. INTRODUCTION

The aim of image processing and image segmentation in this paper is to auto-detecting tuberculosis cavities from the lung X-ray image [1-2]. Therefore, earlier and more certain detection with more effective screening methods can be expected to improve cure rates. The paper presents that to detect tiny tuberculosis cavities from X-ray image, which may present the characteristic of pulmonary tuberculosis and proposes an algorithm that incorporates newer imaging and diagnostic methods to facilitate the evaluation and management of removing the pulmonary tuberculosis cavities.

In the earlier technique of detecting TB, the method was involved with only segmentation using which the

feature extraction was done [10]. The neural network was designed with (100-50-10-2) back progression. This system provided the result as accuracy, sensitivity and specificity at 74.45%, 83.33%, and 66.7% respectively. To increase the result in terms of detecting the TB we adopted another technique along with the existing one. That is we have included enhancement before feature extraction to identify the smallest information available in the lung region to detect TB.

The developed technique involves contrast enhancement using sequentially iterative smoothing filters, histogram equalization, and simultaneous application of two types of edge detection processes namely, maximum-difference edge detection [3] and Canny's edge detection [4]. The post processed image is combined with the original image to accentuate the edges while eliminating noise. Smoothing is implemented because of its effect to reduce specific types of noise signals in the digitized image. However, singular application of smoothing filter does not always provide beneficial results, especially if it is applied to noisy images that are characterized by considerably low signal-to noise ratio. Hence, we proposed an iterative smoothing filter that apply the filter repetitively and obtain series of results for assessment. On the other hand, edge detection aims at increasing the contrast and accentuating the intensity difference. Hybridizing the edge detection with the smoothing filter will increase the contrast, thus help to improve the diagnostic power of the x-ray lung, however different edge detection techniques have varying impact on the resulting images. In this work we have combined two types of image sharpening and edge detection techniques. Figures 1(a) & 1(b) show the block diagrams of the proposed Tuberculosis auto detecting system.

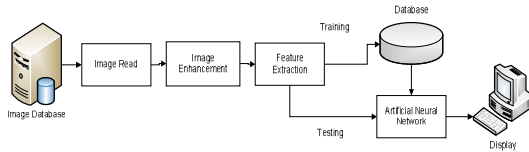


Figure 1

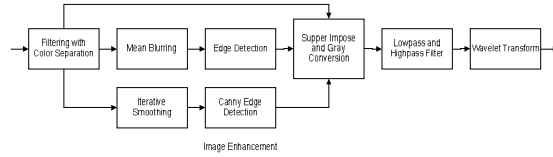


Figure 2

Figure 1 & 2: Block diagrams of the overall proposed system

2. METHODOLOGY

Detecting the tuberculosis cavities from the X-ray image, and that is the target for research. The aim of image processing and image segmentation is to auto-detect tuberculosis cavities, which is one of the most difficult tasks in image processing. Segmentation algorithms for X-ray images generally are based on one of two basic properties of gray-level values: discontinuity and similarity will accord with the requirement [5].

Algorithm I

The proposed repetitive smoothing-sharpening technique employs a number of sequential and also parallel steps. In the first processing step a discrete Laplace high pass operator filter is applied to reduce the noise and enhance the image contrast by eliminating as much noise as possible.

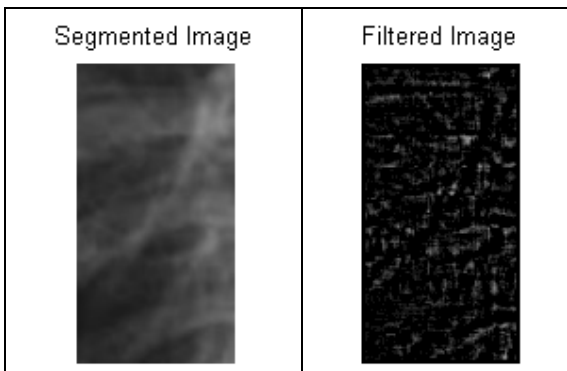


Figure 3: comparison of segmented & filtered X-ray image

Figure 3 shows an example of this step result as applied to x-ray lung samples. The output image from this step is used as input to two individual parallel modules namely Module G and Module B, after performing color separation as shown in Figure 5, where it will undergo further and different processing within these modules and later the outputs are combined with another copy of the image as gained from the first step of the developed technique to produce the enhanced output image. Prior to start modules G and B process, calculation of the standard deviation of the intensities is carried out which is measured as a reflection of contrast R (RMS contrast):

$$\sigma = \sqrt{\frac{1}{MN} \sum_{i=0}^{N-1} \sum_{j=0}^{M-1} (I_{ij} - \bar{I})^2} \quad (1)$$

Where

, M and N are the image number of rows and columns respectively and I is the intensities average value. In module B iterative smoothing is applied to the input image data. The number of repetitions is determined by implementing a preset threshold level of *iteration decision factor H*. The image is smoothed by taking the average of the nine pixel blocks; eight neighboring pixels in addition to the pixel under investigation, Figure 4.

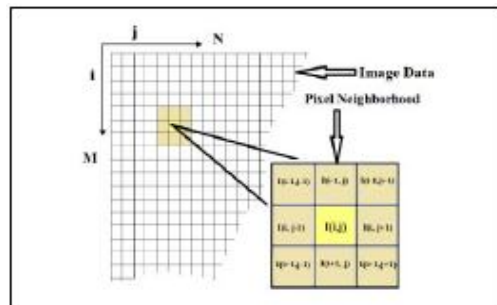


Figure 4: Pixel Neighborhood Representation

The output is then stored into an output array S , hence S is calculated as follow:

$$S(x, y) = [I(i - 1, j - 1) + I(i - 1, j) + I(i - 1, j + 1) + I(i, j - 1) + I(i, j) + I(i, j + 1) + I(i + 1, j - 1) + I(i + 1, j) + I(i + 1, j + 1)] / 9 \quad (2)$$

The S output data array is then used to compute a new σ value by application of Equation 1. A comparison is made between the $(H*\sigma)$ and the new resulting σ value. Additional smoothing step is then repeated if the newly computed σ is $\geq (H*\sigma)$. The same process is repeated till the newly computed value of σ becomes less than the value of $(H*\sigma)$. The main purpose of iterative smoothing is to eliminate as

much as possible of noise from the signal. Although it might seem contra intuitive to smooth an image for contrast increasing, but the proposed and developed technique employ the technique as it balances out the draw back in its next steps resulting in enhanced contrast. The edge array histogram is then equalized using the following equation:

$$\bar{S}(x, y) = \frac{S(i, j) * 255}{Mean(S) + 6 * \sigma(S)} \quad (3)$$

where $Mean(S)$ and $\sigma(S)$ are the mean value and the standard deviation of the resulting intensities in the S array. Canny's edge detection filter [8] is then applied to the filtered image to accentuate contours of the possible *Regions of Interests* (ROIs) that could have been missed by the edge detection in the pathway (i.e. Module G). Whereas Module G applies mean blurring filter to eliminate noise while preserving most of the details. Next the edge attributes in the image data is determined by application of maximum difference of pixel intensity as follow [4].

For each pixel, the difference in intensities between the center point and the 8 neighbors, Figure 4, is determined and the max of those is assigned as the new intensity of the center point in array E:

$$E(i, j) = \max[S(i, j) - S(i - 1, j - 1), S(i, j) - S(i - 1, j), S(i, j) - S(i - 1, j + 1), S(i, j) - S(i, j - 1), S(i, j) - S(i, j + 1), S(i, j) - S(i + 1, j - 1), S(i, j) - S(i + 1, j), S(i, j) - S(i + 1, j + 1)] \quad (4)$$

The average value of the resulting pixels' intensities is determined using the values from the final output of the E array. This computed average is then subtracted from all pixels' intensities (i.e. histogram left-shift). The purpose of this step is to eliminate the background low intensity pixels. The process is calculated as follow:

$$Mean = \sqrt{\frac{1}{MN} \sum_{i=0}^{N-1} \sum_{j=0}^{M-1} E(i, j)} \quad (5)$$

and

$$\bar{E}(i, j) = E(i, j) - Mean \quad (6)$$

Where is the output image data array generated from the intensity subtracting process. Further filtering is applied to isolate resulting edge point that do not have counterpart in the original image.

The three outputs as outlined by Figure 2 flow chart are then superimposed as three bands of RGB domain by assigning the Red-band to the post-Laplacian

image, the Green-band to the filtered and normalized edge detection, and the Blue-band to the Canny's edge Detection contours from sequentially blurred and normalized image. The 24-bit image is then converted into 8-bit grey-scale array as shown in Figure 6, using Pal model to readily enable comparison with the original grey-scale image.

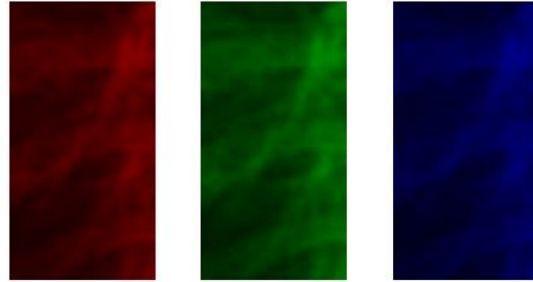


Figure 5 Color Separation of color image

24 bit Enhanced Image 8 bit Enhanced Image

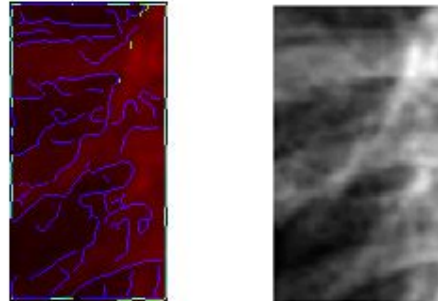


Figure 6. 24-bit color and 8-bit gray color enhancement of proposed algorithm

Algorithm II

The algorithm is expressed as follows:

- (A) Given an initial threshold T (between 64 and 128);
- (B) Using global or local (i.e., adaptive) threshold operator on a gradient magnitude image and getting the high frequency component $h(x, y)$ from the highpass filter;
- (C) Doing edge detection and gaining the observability Image $j(x, y)$;
- (D) Citing the subtraction algorithm to deal with the signals between $j(x, y)$ and $h(x, y)$, and gaining the details of different orientations of image $g(x, y)$ from the wavelets filter.

In the follow section, each step is explained with resultant image. Considering the algorithm (A) and (B), the histogram of typical chest X-ray image is produced. The histogram shows two almost distinct clusters of X-ray numbers. To recover the edges, the

gradient image must be segmented using a global or local (i.e. adaptive) threshold operator. Detecting the tuberculosis cavities from the X-ray image, and that is the target for research. In spite of the characteristic noise, the lowpass filter and high-pass filter could not directly reveal tuberculosis cavities from the image (see Figure 7 (a) (b) (c)). Indeed, the directness of using the filters could not account for this target. However, Laplacian is a derivative operation, which use highlights gray level discontinuities in an image with slowly varying gray level [6]. This will meet our needs whereas, the Canny edge detector [5] is the most rigorously expatiated upon operator, the result is not observability as before (see Figure. 6(d)).

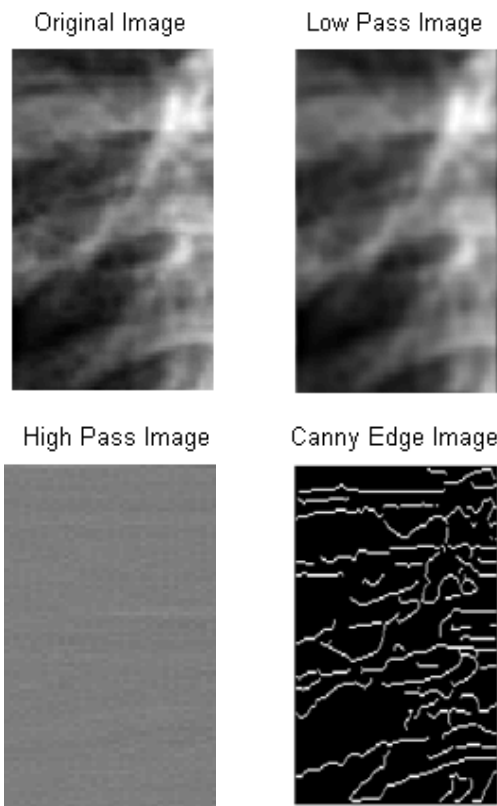


Figure 7. TB cavities detection (a) Image from Algorithm I (b) Low-pass filter detection, (c) The high-pass filter result, (d) Canny edge detection. The key usefulness of Image subtraction is enhancement of difference. It is available to use subtraction algorithm to realize the distributing of the pathological tissue. In this section,

$$\text{When } g(x,y) = f(x,y) - h(x,y) < 0 \quad (7)$$

The value of $g(x, y)$ will be changed as follow:

$$g(x,y) = 0 \text{ and when,} \quad (8)$$

$$(x,y) = f(x,y) - h(x,y) > 0 \quad (9)$$

The value of $g(x, y)$ will not be changed. Therefore, all cases of known or suspected lung cancer or pulmonary tuberculosis should be initially approached with curative intent (see Fig.7 (d)).

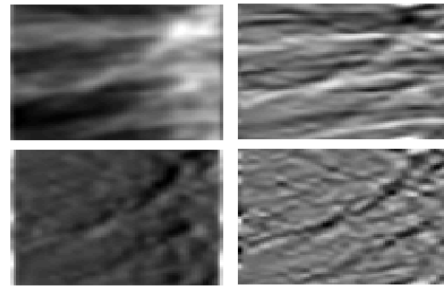


Figure 8. (a) The low-frequency component of Figure 7(d), (b) The horizontal details (a), (c) The diagonal details of (a), and (d) vertical details of (a).

The solitary pulmonary tuberculosis cavities are usually an unexpected finding on a chest film [8]. The wavelets algorithm is aimed to detecting the details of different orientations of object [9]. Based on the features (D) and (E), the octave-band decomposition is used to decompose the low frequency field into more narrow frequency field e (see Figure. 8(a-d)).

For a given project $L^2(R)$, $g_j \in w_j$ and $j \in \mathbb{Z}$, we obtained wavelets decomposition as follow:

$$c_k^{j-1} = \sum_l a_{l-2k} c_l^j \quad (6)$$

$$d_k^{j-1} = \sum_l b_{l-2k} c_l^j \quad (7)$$

Simultaneously, the part of high frequency component is not to keep up decompose. After detection of the early lung cancer X-ray image, most significant information exists in the image.

3. RESULTS

For testing, we used a four-layered BP network (100-50-10-2), including an input layer, an output layer, and a hidden layers, in accordance with TB features. The network was trained by 'traingdm' with 'tansig' activation function for the hidden layer, and 'purelin' linearity function for output. In this process, the target error was 0.003 and the biggest training time was 2000 epochs. Accurate rate, sensitivity, and specificity of our diagnosis were 91.25% (73/80), 90.48% (38/42), and 92.11% (35/38), respectively.

Diagnostic result	Status of disease		Total
	TB	Non-TB	
TB	38	03	41
Non-TB	04	35	39
Total	42	38	80

Table 1: Diagnostic Result of Testing Samples

Comparatively by adding this enhancement method, we have achieved 16.18% of improvement in its accuracy of classification TB.

4. CONCLUSION

The paper presents a novel, wavelet transform based and subtraction algorithm that incorporates newer imaging and diagnostic methods to facilitate the evaluation and management of solitary pulmonary tuberculosis cavities. Management of tuberculosis cavities that are clearly benign or malignant is straightforward. The difficulty is in the evaluation and management of the indeterminate nodule and the goal is to correctly diagnose indeterminate tuberculosis cavities, allowing curative resection of early-stage malignant tuberculosis cavities and avoiding the morbidity and mortality of surgery for benign tuberculosis cavities. From the test results, the proposed technique was successful in detecting tiny cavities on lung X-ray image. This is found to have many advantages over the exiting methods.

Acknowledgement

The authors are very grateful to Mrutyunjaya S. Hiremath, CTO, eMath Technology, India for interesting discussions regarding this work.

REFERENCES

1. A. Jemal, R. Siegel, E. Ward, Y. Hao, J. Xu, and MJ. Thun. **Cancer statistics**, CA Cancer J Clin., Vol.59, pp. 225-249, 2009
2. **World Health Organization WHO “Cancer” Fact sheet** No.297, February 2009, who.int/mediacentre/factsheets/fs297/en/index.html.

3. H. Madjar. **Role of Breast Ultrasound for the Detection and Differentiation of Breast Lesions.** Breast Care 2010;5:109-114 (DOI: 10.1159/000297775)

4. R. F. Chang, C. J. Chen, M. F. Ho, D. R. Chen and WK Moon. **Breast ultrasound image classification using fractal analysis.** Proceedings of the Fourth IEEE Symposium on Bioinformatics and Bioengineering, 2004. BIBE 2004.

5. Y. Guo, H. Cheng, J. Huang, J. Tian, W. Zhao, L. Sun and Y. Su. **Breast ultrasound image enhancement using fuzzy logic,** Ultrasound in Medicine & Biology, Vol.32, Issue. 2, pp. 237-247, Feb 2006.

6. L.E Romans. **Introduction to Computed Tomography,** Springer (1995)

7. R. G. Gonzale and R.E. Woods. **Digital Image Processing,** Addison Wesley, New York (1993).

8. Marr D. and E. Hildreth. **Theory of Edge detection,** Proc. Royal Society of London, vol. B-207, 1980, pp. 187-217.

9. Canny J. **A computational Approach to Edge Detection,** IEEE Trans. Pattern Analysis and Machine Intelligence, Vol. 8, No. 6, 1986, pp. 679-698.

10. Chandrika V, Parvathi C.S and Bhaskar P. **Multifeatured Automatic Tuberculosis Detection System,** Vol 3, No.3 June 2012 Science Publisher U K pp 1601-1605.